RELATIVE SHEAR STRESS DISTRIBUTION IN VEGETATED FLOWS: AN EXPERIMENTAL UNCERTAINTY STUDY

MATEO MUNAR-MARTINEZ [(1)], ANDRÉS VARGAS-LUNA [(2)] & ANDRÉS TORRES [(3)]

[(1)] Master candidate in Hidrosistemas, Pontificia Universidad Javeriana. Bogotá, Colombia. E-mail: munar_williamm@javeriana.edu.co.

[(2)] Associate professor, Pontificia Universidad Javeriana, Bogotá, Colombia. E-mail: avargasl@javeriana.edu.co.

[(3)] Professor, Pontificia Universidad Javeriana, Bogotá, Colombia. E-mail: andres.torres@javeriana.edu.co

ABSTRACT

Vegetation exerts a strong control in the morphological evolution of fluvial systems. It is therefore important to include the effects of vegetation in fluvial studies and numerical models. By assuming a momentum conservation balance, a common way to analyze the flow resistance in vegetated channels splits the total shear stress, τ, into shear stress due to vegetation (or vegetation drag), τ_v, and bed-shear stress, τ_b. However, there are no methodologies available to reduce the contribution of the bed-shear stress, when the vegetation is sparse or dense. To study the latter effect, an intense experimental investigation is carried out. The laboratory experiments are performed in a tilting flume, using rigid vegetation at three different densities and considering emergent and submerged hydraulic conditions. In all the analyzes, the experimental uncertainty was taken into account to improve the representativity of the results obtained. It was found that using the methods without uncertainties can generate errors between 0.1% and 245% and an average error of 62%, compared with the results obtained by considering the propagation of uncertainties. It was possible to develop an equation by PLS to estimate the distribution of shear forces with parameters independent of the flow and representing the characteristics of the vegetation and the channel. This model predicts enough values to represent the process with an error in the estimate of 16%. Our results of this investigation show that the bed-shear stress contribution reduces considerably in configurations where dense vegetation is present.

Keywords: Vegetated flows, shear-stress partitioning, rigid vegetation, laboratory experiments, uncertainty propagation.

1 INTRODUCTION

The presence of vegetation in natural channels affects flow conditions, sediment transport and morphological development of river systems (Hickin, 1984). Field measurements, for example, have shown that vegetation controls riverbanks stability and planform configurations (Kleinhans, 2010). Previous studies have shown that the presence of riparian vegetation can reduce the braiding index of rivers and that vegetation establishment on sediment bars is one of the main factors affecting the migration of river meanders. At larger scales, vegetation also influences the mitigation of floods and sedimentological balances (Gurnell, 2014; Vargas Luna, 2016).

Locally, vegetation increases the resistance to flow, increasing the local hydraulic roughness, generating a decrease in flow velocity and promoting sedimentation (Nepf, 2012). In fact, vegetation alters the vertical velocity profiles, an aspect that radically modifies the hydrodynamics of natural channels (Chen and Kao, 2011; Guo and Zhang, 2016; Tsujimoto, 1999). The effects on velocity profiles depend on the vegetation characteristics and plants height. In relation to water depth, hydrodynamic analyses divide vegetation into two main types: emergent (when vegetation protrudes above the free surface) and submerged (when vegetation is completely below the water surface) (Vargas-Luna et al., 2015).

At present, there exist models that allow estimating the hydraulic roughness of vegetated channels which include separately emergent and submerged conditions and a few models that take into account both cases (Vargas-Luna et al., 2015). All existing models are based on a momentum balance, for uniform flow conditions, described by (Baptist, 2005):

$$\tau = \rho g R_h S = \tau_b + \tau_v \qquad [1]$$

Where τ is the total shear stress (N / m^2), ρ is the density of the fluid (kg / m^3); g is the acceleration due to gravity (m / s^2); R_h is the hydraulic radius (m); S is the channel slope (m / m); τ_b is the bed shear stress (N / m^2) and τ_v is the shear stress absorbed by the vegetation (N / m^2). From equation 1, the reduction of the bed shear stress in a vegetated channel is easily identifiable due to the presence of plants and the associated sedimentation mentioned above.

However, recent research has identified that shear stress distribution may not be applied in a generalized manner (Thompson et al., 2004; Vargas-Luna et al., 2015, 2016). This assumption is supported by considering that the shear stress absorbed by the plants depends on its physical properties (height, diameter, density, etc.) and that an increase of vegetation density results in a reduction of the influence of the bed roughness, aspects that are not considered in equation 1 as the bed shear stress contribution remains constant for any vegetation arrangement. Previous investigations intended to characterize this drag partitioning focused on emergent vegetation, which brings forth the necessity of investigating and characterizing the behavior of submerged vegetation (Thompson et al., 2004). which would furthermore lead to a general description of both hydraulic conditions. For emergent vegetation, the flow velocity is reduced, but the shape of the velocity profile is not substantially modified (see Figure 1a). While in submerged vegetation configuration, the flow velocity is clearly divided into two layers and in the bottom layer (near the bed), the velocity is reduced (see Figure 1b), an aspect that modifies the sediment transport capacity considerably. Understanding better these effects may morphological estimations on vegetated flows.

The existing models to determine each bed shear stress component are based on a factor that modifies the hydraulic roughness coefficient of the bed (Baptist, 2005; Vargas-Luna et al., 2016). This implies the use of a predictor to estimate the global flow resistance and with this, the bed roughness coefficient is calculated. This generates a greater uncertainty in the results by the number of predictors that should be used to estimate all the parameters that the models include.

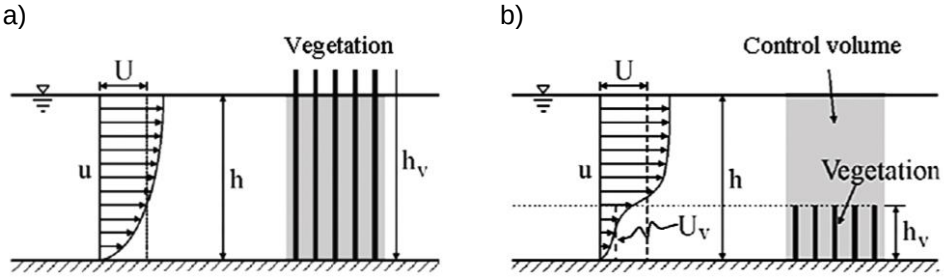

Figure 1. Rigid vegetation in open channels in a) emergent, and b) submerged condition (Wu and He, 2009).

The study of the flow around isolated cylindrical elements began in the early 1950s (eg, Finn, 1953; Tritton, 1959), but only 20 years later cylinder arrays were considered in laboratory experiments to simulate vegetation (Li and Shen, 1973; Petryk and Bosmajian III, 1975; Tollner et al., 1977). These rigid cylinder based contributions helped to identify the relevance of stem density and spatial distribution in flow resistance, flow field and sedimentation processes (see Figure 1b). Other studies showed that the representation of plants as rigid cylinders neglects the reconfiguration of plants under flowing water (Aberle and Järvelä, 2013; Statzner et al., 2006), decreasing the projected area and the drag forces (Albayrak et al., 2014; de Langre et al., 2012; Dittrich et al., 2012; Gosselin et al., 2010; Siniscalchi and Nikora, 2013). However, the most common way to include vegetation in a schematic and easily quantifiable manner in numerical models is through the assumption of rigid cylinder arrays with uniform height, diameter and density (Cheng, 2013; Thompson et al., 2004; Vargas-Luna et al., 2016). Other proposals consider real vegetation including its foliage, but those results can be applied to limited configurations of the characterized species at the considering development stage (Aberle and Järvelä, 2013; Freeman et al., 2000; Järvelä, 2004; Västilä et al., 2013; Velasco et al., 2008). Linking the settings of rigid cylinders to real vegetation is an important unsolved issue. In nature, some plants can be well represented by cylindrical rigid stems but in most cases, it is simply impossible. However, to represent vegetation as rigid cylinders allows to find models that can be replicated since they represent the physics of the process and must be calibrated for each vegetation type.

The objective of this work is to characterize the relative shear stress distribution in vegetated flows through a series of experiments that consider the variation of the hydraulic conditions and the characteristics of the plants. Given the versatility and correspondence with the existing mathematical models, rigid and cylindrical elements will be used as vegetation, varying their height and density. The results bring forth advances on the understanding of the relative contribution of shear stresses on the bed and those absorbed by the vegetation and will lead to understanding better the interaction between the two components, from simplified parameters and independent of the hydraulic properties of the flow. These advances allow a simplified description of the effects of vegetation on the morphological response of natural channels as a range of distribution of shear stress, an aspect of vital relevance in various disciplines such as fluvial morphodynamics, eco-hydraulics, river engineering, among others.

2 MATERIALS AND METHODS

2.1 Experimental setup

The experiments were conducted in conditions of uniform flow, in a tilting flume 9.0 m long, 0.3 m wide and 0.4 m deep (see Figure 2), of the hydraulics laboratory of the Pontificia Universidad Javeriana. The flume has glass walls and steel bottom. The flow was controlled through the use of a valve and measured by an ultrasonic meter flow, this has an accuracy of 0.1 liters per second, while the flow depth was adjusted using a gate located at the downstream end of the channel. The water level was measured at six points with a SIEMENS ultrasonic level sensor, providing a continuous measurement with 1 millimeter precision and accuracy of 0.15% of the measured value. The velocity measurements were carried out with a high-resolution ADV velocimeter (Acoustic Doppler Velocimeter - 3D), Vectrino NORTEK (which allows continuous measurement in three dimensions and accuracy of 0.5% of the measured value ± 1 mm/s).

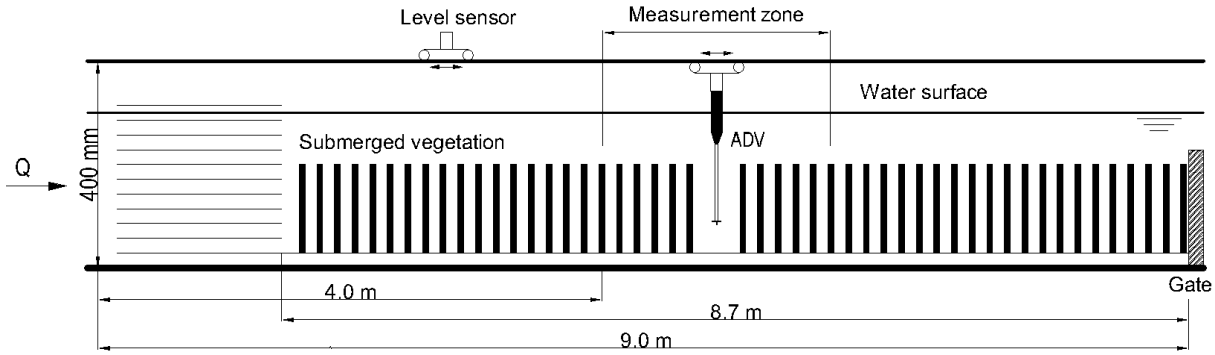

Figure 2. Experimental setup - flume side view.

In the measurement zone, located four meters downstream the entrance of the channel (see Figure 2), two cylinders were removed to allow the positioning of the velocity measuring device. Previous investigations have shown that the impact of the elimination of the cylinders on the measured velocity can be insignificant over such a short distance (Ghisalberti and Nepf, 2004; Ikeda and Kanazawa, 1996; Velasco et al., 2008). The bottom of the flume was covered by a false modular wooden bed, *Clathrotropis brunnea*, 38 mm high, covered with glued fine gravel on which the vegetation was located.

Table 1. Summary of the hydraulic conditions and the vegetation configurations.

Test N°	Hydraulic condition	h_v [m]	h [m]	Density [λ]	S [m/m]	Test N°	Hydraulic condition	h_v [m]	h [m]	Density [λ]	S [m/m]
1	EV	0.300	0.300	0.009	0.0001	**22**	EV	0.30	0.075	0.009	0.0010
2	EV	0.300	0.300	0.024	0.0001	**23**	EV	0.30	0.075	0.024	0.0010
3	EV	0.300	0.300	0.033	0.0001	**24**	EV	0.30	0.075	0.033	0.0010
4	EV	0.300	0.300	0.009	0.0010	**25**	SV	0.15	0.3	0.009	0.0001
5	EV	0.300	0.300	0.024	0.0010	**26**	SV	0.15	0.3	0.024	0.0001
6	EV	0.300	0.300	0.033	0.0010	**27**	SV	0.15	0.3	0.033	0.0001
7	EV	0.300	0.150	0.009	0.0001	**28**	SV	0.15	0.3	0.009	0.0010
8	EV	0.300	0.150	0.024	0.0001	**29**	SV	0.15	0.3	0.024	0.0010
9	EV	0.300	0.150	0.033	0.0001	**30**	SV	0.15	0.3	0.033	0.0010
10	EV	0.300	0.150	0.009	0.0010	**31**	SV	0.10	0.3	0.009	0.0001
11	EV	0.300	0.150	0.024	0.0010	**32**	SV	0.10	0.3	0.024	0.0001
12	EV	0.300	0.150	0.033	0.0010	**33**	SV	0.10	0.3	0.033	0.0001
13	EV	0.300	0.100	0.009	0.0001	**34**	SV	0.10	0.3	0.009	0.0010
14	EV	0.300	0.100	0.024	0.0001	**35**	SV	0.10	0.3	0.024	0.0010
15	EV	0.300	0.100	0.033	0.0001	**36**	SV	0.10	0.3	0.033	0.0010
16	EV	0.300	0.100	0.009	0.0010	**37**	SV	0.08	0.3	0.009	0.0001
17	EV	0.300	0.100	0.024	0.0010	**38**	SV	0.08	0.3	0.024	0.0001
18	EV	0.300	0.100	0.033	0.0010	**39**	SV	0.08	0.3	0.033	0.0001
19	EV	0.300	0.075	0.009	0.0001	**40**	SV	0.08	0.3	0.009	0.0010
20	EV	0.300	0.075	0.024	0.0001	**41**	SV	0.08	0.3	0.024	0.0010
21	EV	0.300	0.075	0.033	0.0001	**42**	SV	0.08	0.3	0.033	0.0010

* EV - Emergent vegetation & SV - Submerged vegetation.

The vegetated area was 8.70 m long, using as vegetation surrogates rigid wood cylinders, *Jacarnda copaia*, with a diameter of 9.5 mm. The cylinders were arranged in a staggered configuration, defining three different dimensionless densities (λ= 0.009, 0.024 and 0.033) defined by equation 2.

$$\lambda = \frac{m\pi D^2}{4} \quad [2]$$

Where m is the number of elements [m^{-2}] and D is the diameter of each cylinder [m]. For each test with emergent vegetation, a constant vegetation height of h_v=0.3 m and four flow depths h = 0.075, 0.1, 0.15 and 0.3 m were considered. Conversely, in the tests with submerged vegetation, a 0.3 m water depth was maintained and three vegetation heights were considered, h_v = 0.075, 0.1, 0.15 m. Forty-two tests with vegetation were carried out and are summarized in Table 1.

2.2 Experimental procedure

For each experiment, a period for setting the initial configuration was required. The false bed was installed on the bottom of the flume and the cylinders were put in the configuration and density for each test. The water depth was measured with the level sensor and a ruler with an accuracy of half a millimeter along the channel in control sections, spaced 1 m apart. Once the uniform flow condition was reached, the vertical velocity profile was obtained, performing the measurements every 0.5 centimeters, from the first 5 centimeters counted from the bed (The ADV doesn't estimate the velocity at lower water depths). The duration of the flow velocity measurement was defined in preliminary stages of the adjustment of the equipment. A convergence analysis determined that a sufficient volume of information to perform the subsequent data analysis is obtained when measuring at a frequency of 200 Hz for 50 seconds and, therefore, collecting 10,000 data approximately per point. A similar procedure was used by Tang et al (2014).

2.3 Data analysis

Since the variables considered are experimental, they have uncertainty due to the limitations of the measurement, for example, due to the precision of the instruments. It is well know that the errors of each variable involved in the calculation of a function is propagated and affects its accuracy and precision. To obtain an equation that captures all the possible values of the reduction factor of the shear stress on the bed, f, was calculated, which relates the shear stress on the bed and the total shear stress in vegetated flows, see equation 3. A propagation of uncertainty was carried out using the Monte Carlo method, based on all the variables and parameters considered in the experimental tests, including the flow velocity, the water depth, the channel slope, and height, diameter and density of vegetation.

$$f = \frac{\tau_b}{\tau} \quad [3]$$

A non-invasive filter is applied to the obtained velocity profiles to eliminate the values that the ADV reports as noise. Assuming a normal distribution with the first moment in the measured value and a second moment as half of the equipment's precision (standard uncertainty), synthetic velocity profiles were generated. Following the same methodology, synthetic temperature series were generated. The atmospheric pressure and acceleration of gravity adjusted for Bogota, altitude of 2640 m, are calculated using Equations 4 (National oceanic and atmospheric administration, 1976) and 5 (Serway and Jewett, 2018), respectively. Synthetic series of the water temperature were used to calculate the density (Equation 6 (Engineering ToolBox, 2009)), the specific gravity (Equation 7 (Engineering ToolBox, 2009)) and the kinematic viscosities of the water (Equation 9 (Engineering ToolBox, 2009)) for each test. The flow in the tests was uniform flow, i.e. the flow depth is the same in all sections of the channel. However, due to the precision of the instrument used to measure the depth of the flow, synthetic series of the depth of the flow were generated.

$$P(z) = P_0 e^{-\alpha z} \quad [4]$$

$$g_z = g_0 \left(\frac{r_e}{r_e + z}\right)^2 \quad [5]$$

Where $P(z)$ is the atmospheric pressure at a height z in Pa, P_0 is the reference pressure at sea level (101.325 Pa), α is the decay density constant (1,186 x10^{-4} m^{-1}), g_z is the acceleration due to gravity at height z, with respect to sea level (m/s^2), r_e, is the average radius of the Earth (6.371.000 m) and g_0 is the acceleration due to gravity at sea level (m/s^2).

$$\rho_{H_2O} = \frac{\rho_0/(1 + \beta * (T - T_0))}{1 - (P - P_0)/E} \quad [6]$$

$$\gamma_{H_2O} = \rho_{H_2O} * g \quad [7]$$

$$\mu = 2.414 * 10^{-5} * 10^{247.8 / ((T + 273.15) - 140)} \quad [8]$$

$$\nu = \frac{\mu}{\rho_{H_2O}} \quad [9]$$

Where ρ_{H_2O} is the density of water (kg/m^3), β is the coefficient of expansion of water (0.000088 m^3/m^3°C), T is the water temperature (°C), To is the temperature in the reference at sea level (°C), P is the atmospheric pressure (Pa), Po is the atmospheric pressure in the reference at sea level (Pa), E is the water volume module (2.15x10^9 N/m^2), γ_{H_2O} is the specific weight of water (N/m^3), g is the acceleration due to gravity (m/s^2), μ is the dynamic viscosity of water (N·s/m^2) and ν is the kinematic viscosity of water (m^2/s).

The channel slope was estimated as the vertical difference divided by the horizontal difference. The vertical difference was measured at two points with an accuracy of 0.0005 m, while the horizontal difference was established at 5 meters with an accuracy of 0.001 m. The uncertainty associated with measuring the channel slope at each of the three measurement points was propagated. Random numbers were generated in each of these, following a normal distribution with mean equal to the measured value and deviation equal to half of the precision of the instrument. With this random data, synthetic series of the channel slope was calculated for each test.

A convergence analysis of the average diameter and average height of the cylinders is performed to represent the vegetation. The diameter and height of the randomly selected cylinders were measured with an accuracy of 0.00002 m and 0.0005 m, respectively. The point of convergence of average diameter and average height was identified when the variation of this was equal to the pressure of the instrument with which it was measured. With these data, synthetic series of diameter and height of vegetation were generated.

To determine the number of synthetic generations needed to capture the physics of all tests, a convergence analysis of the variables and parameters considered was carried out. The variation of the average of the variables was evaluated according to the number of synthetic generators. It was established that the convergence is reached when the variation of the average of the variable is less than the instrument with which it was measured, this allowed determining that 1000 synthetic generations are enough.

The average flow velocity in the vegetation zone was estimated from each velocity profile. From the mean velocity, the Reynolds number representative of this area was calculated and used to estimate the resistance due to the bed material in terms of Chezy roughness coefficient, using Equation 10 (Vargas-Luna et al., 2015b). This equation was obtained experimentally under conditions like those of our experiments, estimating the roughness coefficient of the bed as a function of the channel slope and the Reynolds number. An uncertainty propagation exercise was carried out from the data, obtaining 1000 sets of coefficients that solve equation 10, summarized in Table 2.

$$C_b = X1 * Re^{X2} + S^{X3} \quad [10]$$

Table 2. Parameters considering the uncertainty of equation 6.

	X1	X2	X3
Min	0.5207340	0.2914364	-0.1839737
Median	0.5220189	0.2916028	-0.1838543
Max	0.5232896	0.2917484	-0.1837207

After calculating the hydraulic roughness due to the bed material C_b, the shear stresses on the bed for the cases including vegetation (τ_b) were estimated by equation 11, assuming uniform flow conditions.

$$\tau_b = \frac{\rho g}{{C_b}^2} {u_v}^2 \quad [11]$$

Where ρ is the density of the fluid (kg / m^3); g is the acceleration due to gravity (m / s^2); C_b is the coefficient of flow resistance of the bed in a Chezy form (m$^{1/2}$/s) and u_v is the mean flow velocity in the vegetation zone (m/s). The total shear stress was estimated using equation 1. With the two shear stresses, the reduction factor of the shear stress on the bed, f, was calculated using equation 3.

The Partial Least Squares regression named hereafter PLS is used. PLS, cited by Torres and Bertrand-Krajewski (2008), generalizes and fuses the principal component analysis (PCA) and multiple regression methods. It is especially useful in cases where the number of variables is comparable to or greater than the number of observations and/or where exist other factors leading to correlations between variables (Torres et al., 2013; Torres and Bertrand-Krajewski, 2008).

The PLS was used with the R software to estimate an equation expressing the channel slope (m/m), the density of the vegetation (λ) and the submergence ratio (h/h_v). The shape of the equation that is found when using the PLS is that described in Equation 12. The process of calibrating the coefficients $X1$, $X2$, $X3$ and $X4$ was done 1000 times, each with a set of parameters of 42 tests, the data were randomly divided into two groups, two thirds of the data to perform the calibration process and a third to perform the validation.

$$f = X1 + X2 * \left(\frac{h}{h_v}\right) + X3 * S + X4 * \lambda \quad [12]$$

To quantify and evaluate the estimation performance of the equation, this method uses the normalized RMSE (NRMSE) (Equation 13), which relates the RMSE to the observed range of the variable. Thus, the NRMSE can be interpreted as a fraction of the overall range that is typically resolved by the model. NRMSE is a measure of accuracy, to compare predicted errors of different models between dataset.

$$NRMSE = \frac{RMSE}{x_{max} - x_{min}} \quad [13]$$

A cross-validation exercise was performed to evaluate the performance of the prediction of each of the coefficient sets of Equation 12 with data unrelated to its calibration. We used 999 data sets different from the one used for the calibration of the model and a set of mean values, calculated without considering the uncertainty in the data and average properties of the flow and vegetation. We estimated the average error of each model from the NRMSE of the 999 estimates made with each model. The best model and the range of cross-validation errors were established.

3 RESULTS

Figure 3 shows the synthetic velocity profiles generated from the measurements of the tests with flow depth *h*=0.3m. In this figure, one can observe a change in the way in which the velocity profile is developed. When the vegetation is emergent ($h/h_v < 1$), the velocity has a vertical development and few variations are observed in the medium profile and its confidence interval. In other words, bottom velocities are not significantly different from surface velocities, Wilcoxon p-value>0.05 (p-value = 0.42, 0.09 and 0.07 respectively for the three densities). Conversely, the profile developed in configurations with vegetation in submerged condition ($h/h_v > 1$) is divided into two phases. The first is developed in the area where the vegetation is located; it has a vertical development very similar to that presented in emergent condition. The second phase develops above the vegetation zone. A logarithmic velocity profile is developed, similar to developed in free flow conditions. It was found that the velocities of the two phases are significantly different, p-value <0.05 (0.008 and 0.012 respectively for tests with a vegetation height of 0.1 m and 0.075 m).

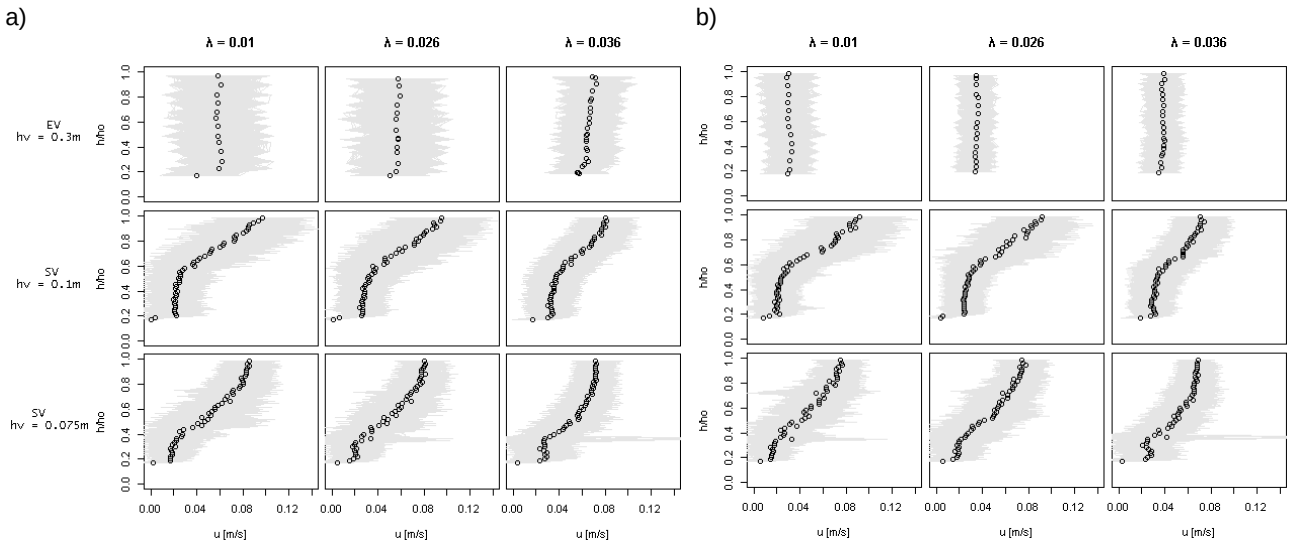

** EV - Emergent vegetation & SV - Submerged vegetation.*

Figure 3. Velocity profiles for a channel slope of a) 0.001 m/m and b) 0.0001 m/m

In an emergent condition, it is evident how the increase in vegetation density contracts the median profile and increases the band of uncertainty in the velocity profile. It was found that the changes of the mean velocity in response to the change of vegetation density are significant (p-value = 0.03 and 0.001, between the densities of 0.01-0.026 and 0.026-0.036, respectively). The differences between the band of the uncertainty of the velocity profile between the densities of 0.01-0.026 are not significant (p-value = 0.3), while between the densities of

0.026-0.036, the differences are significant (p-value = 0.008). In submerged condition, it is observed that the increase in vegetation reduces the average flow velocity in the vegetation zone but increases the gradient of the velocity between the two zones. The increase of the vegetation density produces a lower vegetation velocity and the velocity profile that develops in the upper part has a greater magnitude. The differences between the velocities of the two phases of the velocity profile are significant (Wilcoxon p-value of 0.008 and 0.012, for vegetation heights of 0.1 and 0.075 m, respectively). In the same way, the increase of the slope generates an increase not significant (p-value> 0.05) of the velocity magnitude and its band of uncertainty.

In the velocity profiles with vegetation of 0.075 m, it is observed that between the transition of the two phases of the profile, there is a zone of turbulence with significantly different velocities than those presented in the vegetated zone (p-value = 0.00003) and that the superficial velocities (p-value = 0.000002).

Table 3 summarizes the median values and their confidence interval of each variable obtained from the uncertainty propagation analysis. The values contained in this table are the vegetation submergence ratio, h / h_v, the channel slope, S, the dimensionless density of the vegetation, λ, the average flow velocity in the vegetation zone, u_v, the shear stress, τ, the shear stress on the bed, τ_b, the shear stress absorbed by the vegetation, τ_v, and the reduction factor of the shear stress on the bed, f.

Table *3.* Summary of Results.

h/hv	S [m/m]	Density (λ)	U_v [m/s]	τ [N/m²]	τ_b [N/m²]	τ_v [N/m²]	*f*
1.001 ± 0.004	1.0.E-04 ± 6.3E-05	0.036 ± 0.001	0.0217 ± 0.016	0.099 ± 0.060	0.004 ± 0.004	0.095 ± 0.058	0.035 ± 0.038
0.999 ± 0.004	1.0.E-03 ± 2.6E-05	0.036 ± 0.001	0.0177 ± 0.014	0.977 ± 0.024	0.006 ± 0.007	0.971 ± 0.026	0.006± 0.006
1.000 ± 0.004	9.9.E-05 ± 7.0E-05	0.026 ± 0.001	0.0314 ± 0.013	0.096 ± 0.068	0.006 ± 0.004	0.090 ± 0.067	0.062± 0.041
1.000 ± 0.004	1.0.E-03 ± 2.5E-05	0.026 ± 0.000	0.0298 ± 0.023	0.978 ± 0.024	0.013 ± 0.013	0.965 ± 0.027	0.013± 0.013
1.000 ± 0.004	1.0.E-04 ± 6.4E-05	0.010 ± 0.000	0.0313 ± 0.015	0.099 ± 0.063	0.006 ± 0.004	0.093 ± 0.059	0.060± 0.046
1.000 ± 0.004	1.0.E-03 ± 2.4E-05	0.010 ± 0.000	0.0719 ± 0.031	0.979 ± 0.023	0.045 ± 0.027	0.934 ± 0.035	0.046± 0.029
0.500 ± 0.004	9.9.E-05 ± 6.3E-05	0.036 ± 0.001	0.0214 ± 0.013	0.075 ± 0.047	0.003 ± 0.003	0.071 ± 0.044	0.049± 0.045
0.498 ± 0.004	1.0.E-03 ± 2.6E-05	0.036 ± 0.001	0.0468 ± 0.028	0.734 ± 0.021	0.024 ± 0.020	0.710 ± 0.025	0.032± 0.026
0.499 ± 0.004	1.0.E-04 ± 6.3E-05	0.026 ± 0.001	0.0342 ± 0.010	0.072 ± 0.044	0.007 ± 0.004	0.066 ± 0.044	0.093± 0.053
0.500 ± 0.004	1.0.E-03 ± 2.6E-05	0.026 ± 0.001	0.0367 ± 0.017	0.733 ± 0.019	0.017 ± 0.011	0.716 ± 0.025	0.023± 0.014
0.499 ± 0.004	1.0.E-04 ± 6.6E-05	0.010 ± 0.000	0.0384 ± 0.016	0.075 ± 0.045	0.008 ± 0.005	0.067 ± 0.044	0.109± 0.076
0.497 ± 0.004	1.0.E-03 ± 2.6E-05	0.010 ± 0.000	0.0690 ± 0.021	0.734 ± 0.020	0.042 ± 0.019	0.691 ± 0.025	0.057± 0.025
0.332 ± 0.004	9.9.E-05± 6.5E-05	0.036 ± 0.001	0.0170 ± 0.007	0.058 ± 0.038	0.002 ± 0.002	0.055 ± 0.037	0.043± 0.030
0.333 ± 0.004	1.0.E-03 ± 2.6E-05	0.036 ± 0.001	0.0534 ± 0.019	0.587 ± 0.016	0.030 ± 0.015	0.557 ± 0.024	0.050± 0.027
0.332 ± 0.004	1.0.E-04± 6.8E-05	0.026 ± 0.001	0.0227 ± 0.007	0.059 ± 0.040	0.004 ± 0.002	0.056 ± 0.038	0.065± 0.038
0.332 ± 0.004	1.0.E-03 ± 2.7E-05	0.026 ± 0.001	0.0456 ± 0.014	0.587 ± 0.016	0.024 ± 0.010	0.563 ± 0.017	0.041± 0.016
0.332 ± 0.004	9.8.E-05± 6.9E-05	0.010 ± 0.000	0.0284 ± 0.007	0.057 ± 0.036	0.005 ± 0.002	0.052 ± 0.033	0.092± 0.050
0.333 ± 0.004	1.0.E-03 ± 2.6E-05	0.010 ± 0.000	0.0621 ± 0.015	0.587 ± 0.014	0.036 ± 0.011	0.550 ± 0.016	0.062± 0.020
0.250 ± 0.004	1.0.E-04± 6.8E-05	0.036 ± 0.001	0.0301 ± 0.007	0.049 ± 0.031	0.006 ± 0.002	0.044 ± 0.031	0.119± 0.063
0.249 ± 0.004	1.0.E-03 ± 2.7E-05	0.036 ± 0.001	0.0557 ± 0.012	0.489 ± 0.015	0.031 ± 0.010	0.458 ± 0.019	0.064± 0.021
0.249 ± 0.004	1.0.E-04± 6.7E-05	0.026 ± 0.001	0.0348 ± 0.005	0.049 ± 0.033	0.007 ± 0.002	0.0 ± 0.032	0.142± 0.059
0.250 ± 0.004	1.0.E-03 ± 2.6E-05	0.026 ± 0.001	0.0556 ± 0.012	0.489 ± 0.014	0.031 ± 0.009	0.458 ± 0.018	0.064± 0.018
0.250 ± 0.004	1.0.E-04± 6.7E-05	0.010 ± 0.000	0.0375 ± 0.005	0.049 ± 0.028	0.008 ± 0.002	0.041 ± 0.027	0.156± 0.064
0.250 ± 0.004	1.0.E-03 ± 2.7E-05	0.010 ± 0.000	0.0647 ± 0.008	0.489 ± 0.013	0.039 ± 0.007	0.450 ± 0.015	0.079± 0.013
2.004 ± 0.023	1.0.E-0± 7.1E-05	0.036 ± 0.001	0.0135 ± 0.001	0.099 ± 0.070	0.003 ± 0.001	0.096 ± 0.069	0.028± 0.012
2.003 ± 0.023	1.0.E-03 ± 2.6E-05	0.036 ± 0.001	0.0033 ± 0.001	0.978 ± 0.026	0.001 ± 0.000	0.978 ± 0.026	0.001± 0.000
2.004 ± 0.022	1.0.E-04± 6.8E-05	0.026 ± 0.001	0.0061 ± 0.001	0.098 ± 0.066	0.001 ± 0.000	0.097 ± 0.065	0.009± 0.005
2.004 ± 0.022	1.0.E-03 ± 2.7E-05	0.026 ± 0.001	0.0069 ± 0.001	0.978 ± 0.027	0.002 ± 0.000	0.976 ± 0.026	0.002± 0.000
2.004 ± 0.022	1.0.E-04± 6.9E-05	0.010 ± 0.000	0.0275 ± 0.001	0.098 ± 0.067	0.007 ± 0.002	0.090 ± 0.064	0.076± 0.030
2.004 ± 0.022	1.0.E-03 ± 2.6E-05	0.010 ± 0.000	0.0305 ± 0.001	0.980 ± 0.025	0.020 ± 0.001	0.960 ± 0.025	0.021± 0.001
3.005 ± 0.046	1.0.E-04± 6.9E-05	0.036 ± 0.001	0.0134 ± 0.002	0.099 ± 0.068	0.003 ± 0.002	0.096 ± 0.067	0.033± 0.021
3.007 ± 0.043	1.0.E-03 ± 2.6E-05	0.036 ± 0.001	0.0146 ± 0.001	0.979 ± 0.024	0.009 ± 0.001	0.969 ± 0.025	0.009± 0.001
3.006 ± 0.046	1.0.E-04± 6.9E-05	0.026 ± 0.001	0.0130 ± 0.002	0.097 ± 0.064	0.003 ± 0.001	0.094 ± 0.063	0.031± 0.020
3.006 ± 0.045	1.0.E-03 ± 2.6E-05	0.026 ± 0.001	0.0125 ± 0.001	0.978 ± 0.025	0.007 ± 0.001	0.971 ± 0.025	0.007± 0.001
3.006 ± 0.044	1.0.E-04± 6.6E-05	0.010 ± 0.000	0.0210 ± 0.005	0.099 ± 0.067	0.007 ± 0.002	0.092 ± 0.061	0.068± 0.042
3.005 ± 0.045	1.0.E-03 ± 2.7E-05	0.010 ± 0.000	0.0207 ± 0.001	0.979 ± 0.026	0.015 ± 0.001	0.965 ± 0.027	0.015± 0.002
4.007 ± 0.078	1.0.E-04± 6.6E-05	0.036 ± 0.001	0.0150 ± 0.003	0.100 ± 0.065	0.005 ± 0.002	0.095 ± 0.064	0.048± 0.023
4.008 ± 0.074	1.0.E-03± 2.7E-05	0.036 ± 0.001	0.0163 ± 0.001	0.979 ± 0.027	0.012 ± 0.001	0.966 ± 0.027	0.013± 0.002
4.006 ± 0.073	1.0.E-04± 6.3E-05	0.026 ± 0.001	0.0138 ± 0.002	0.099 ± 0.060	0.004 ± 0.001	0.095 ± 0.059	0.042± 0.019
4.006 ± 0.072	1.0.E-03± 2.7E-05	0.026 ± 0.000	0.0156 ± 0.001	0.978 ± 0.026	0.012 ± 0.002	0.966 ± 0.026	0.012± 0.001
4.007 ± 0.071	1.0.E-04± 6.4E-05	0.010 ± 0.000	0.0233 ± 0.003	0.098 ± 0.059	0.009 ± 0.003	0.090 ± 0.060	0.089± 0.040
4.007 ± 0.072	1.0.E-03± 2.6E-05	0.010 ± 0.000	0.0228 ± 0.003	0.979 ± 0.025	0.020 ± 0.004	0.959 ± 0.025	0.020± 0.004

Table 3 shows how the distribution of shear stresses in vegetated flows is influenced by the submergence ratio. The shear stress absorbed by the vegetation increases as the submergence ratio, presenting the least shear stress on the bed when the vegetation is submerged. By analyzing the distribution of the shear stresses as a function of the submergence relation, it is possible to demonstrate the existence of trend relationships that allow the data to be grouped according to the combinations of the channel slope and the density of the vegetation.

Figure 4 was constructed from the data contained in Table 3 and represents the behavior of the reduction factor of the shear stress on the bed as a function of the vegetation submergence ratio for each combination, the density of vegetation, and the channel slope. In Figures 4a, 4b and 4c it can be seen how the cut-off reduction factor f behaves inversely proportional to the vegetation density. Two dominant slopes are presented in the behavior of f that represent the hydraulic condition of the vegetation, emergent and submerged. It is observed how the slope is a conditioner of the magnitude but not of the behavior of the reduction factor of the shear stress on the bed. The trend form of the median values does not change between the high and low slopes, while their magnitude and confidence interval increase proportionally with the slope.

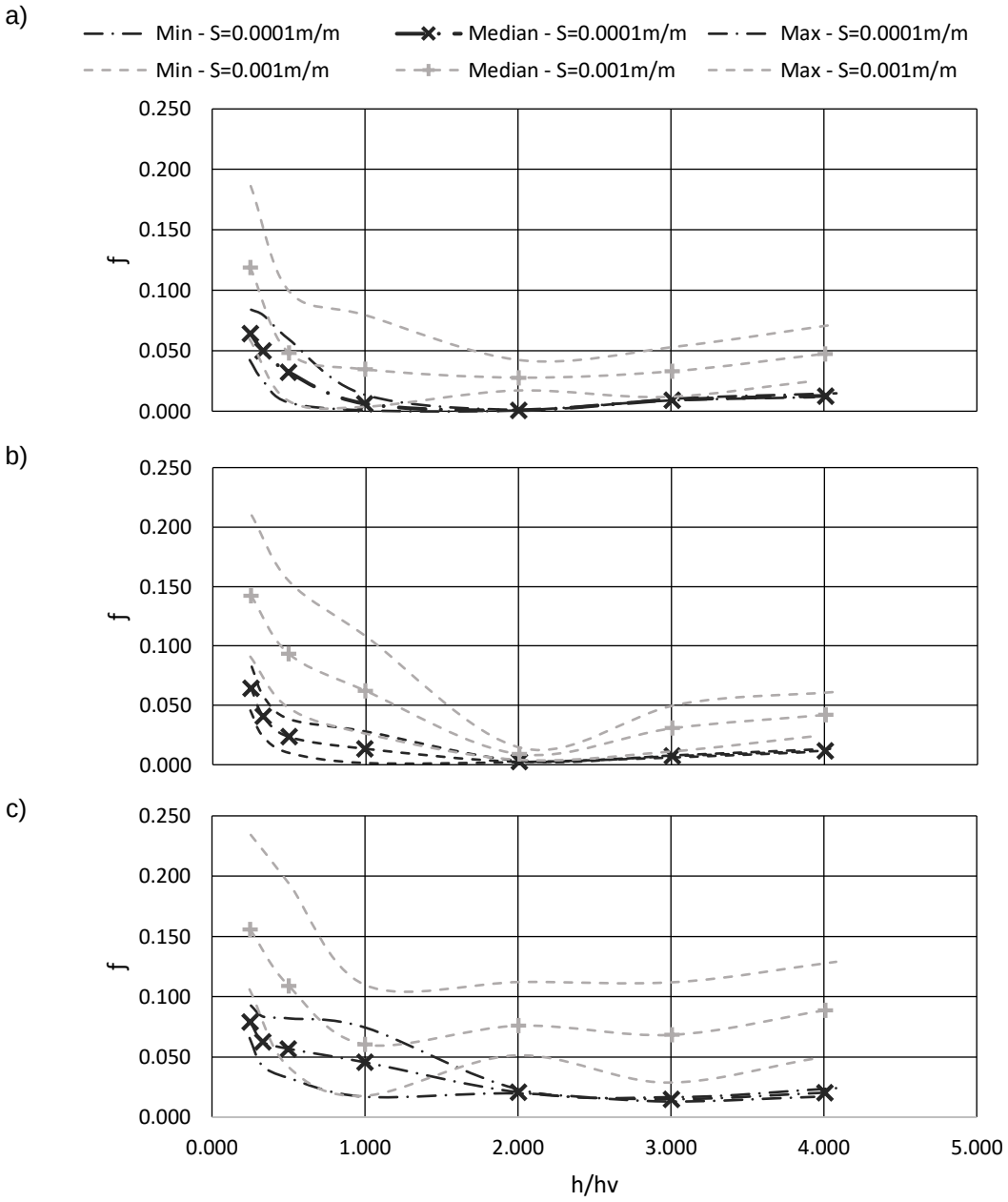

Figure 4. Reduction factor, f, as a function of the submergence ratio, a) $\lambda = 0.036$, b) $\lambda = 0.026$ y c) $\lambda = 0.01$.

For the emergent case, the shear stress absorbed by the vegetation is less than the absorbed in the submerged condition, the shear stress absorbed by the vegetation reduces directly proportional to the submergence ratio. This demonstrates that tall vegetation with small depth flow does not present large reductions in shear stress,

such as large trees and shrubs encountered in floodplains. Conversely, vegetation in submerged condition generates greater protection and absorbs more shear stress. The confidence interval of the reduction factor is lower on low slopes (less than 0.0005 m / m) than on steep slopes (larger than 0.0005 m / m).

From the 1000 sets of the 42 measurements of submergence ratio, the channel slope, the density of the vegetation and the factor of reduction of the shear stress on the bed, a thousand sets of coefficients $X1$, $X2$, $X3$ and $X4$ were calibrated and validated with the PLS (Equation 12). Table 4 presents the occurrence ranges of coefficients and the calibration and validation errors with a probability of occurrence of 95%.

Table *4.* Parameters with uncertainty, calibration error and validation of equation 12 and best model.

	X1	X2	X3	X4	NRMSE - CAL	NRMSE - VAL
Min	0.08834	-0.01984	-69.84884	-2.23176	11.7 %	9.9 %
Median	0.12530	-0.01290	-45.02119	-1.21990	16.2 %	21.4 %
Max	0.16042	-0.00560	-21.61935	-0.25860	20.9 %	34.9 %
Best Model	0.11227	-0.00908	-51.98437	-0.58823		16.06 %

A cross-validation exercise was carried out to evaluate the performance of each one of the 1000 equations obtained by the PLS. The models were evaluated with 999 data sets and a set of average values obtained without performing an uncertainty propagation analysis. From this analysis, it was possible to determine the best model, whose coefficients are presented in Table 4, with an average normalized error of 16%. The average error of cross-validation of all the models fluctuates between 16.068% and 16.077%, presenting an average value of 16.073%.

To evaluate the best model with all the generated models, its prediction was assessed with the mean values of the 42 measurements, because these were not included in the calibration process. Figure 5 presents the distribution of the predictions of the thousand models from the mean values, the estimations made by the best model and the average value observed are highlighted. It's observed that the prediction of factor f of some of the 42 tests is overestimated by most models.

Given the disparity found between the mean values and values with uncertainty, and the overestimation of the prediction in some tests, the incidence of the propagation of the uncertainty on the measured data and its variation with the mean values, estimated from the uniform flow, was evaluated. Figure 5b shows a comparison between the reduction median value of factor, f, of the shear stress on the bed, considering the uncertainties and the observed mean values. It's observed how the factor f calculated with uncertainty presents higher values than those that do not consider it. The analysis of uncertainty propagation considered the variations in water temperature during the measurements, which condition their properties (density and viscosity). Contrary to the results obtained from the uncertainty analysis, the average values were estimated using the method without uncertainty, in this the results were estimated from the average properties of the flow. In addition, the uncertainty analysis considers the variations associated with the instrument and due to the environment. Therefore, it can be considered that the values obtained by the method of propagation of uncertainty are more trustworthy than those obtained by the method with mean values. It was found that using the methods without uncertainties can generate errors between 0.1% and 245% and an average error of 62%, compared with the results obtained by considering the propagation of uncertainties (Figure 5b).

a)

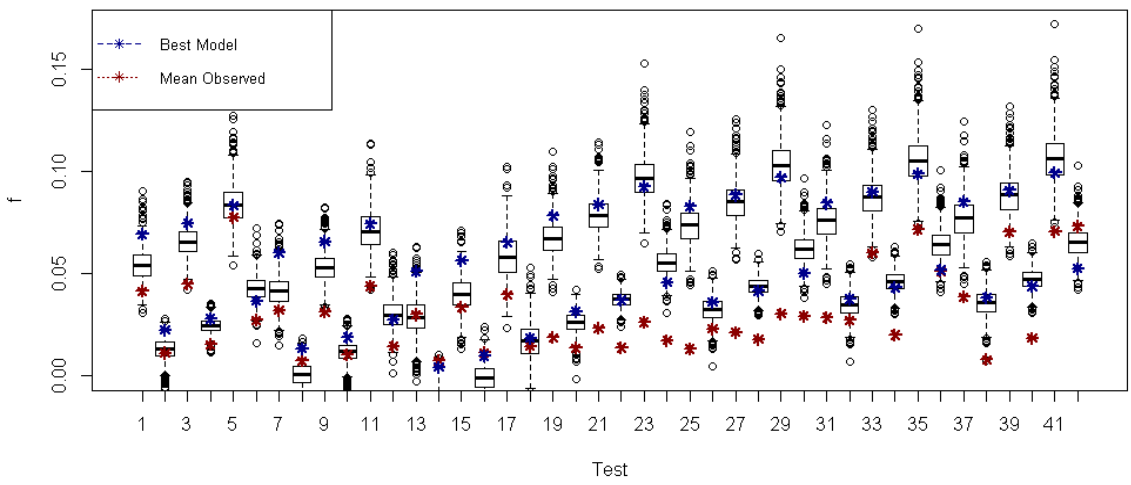

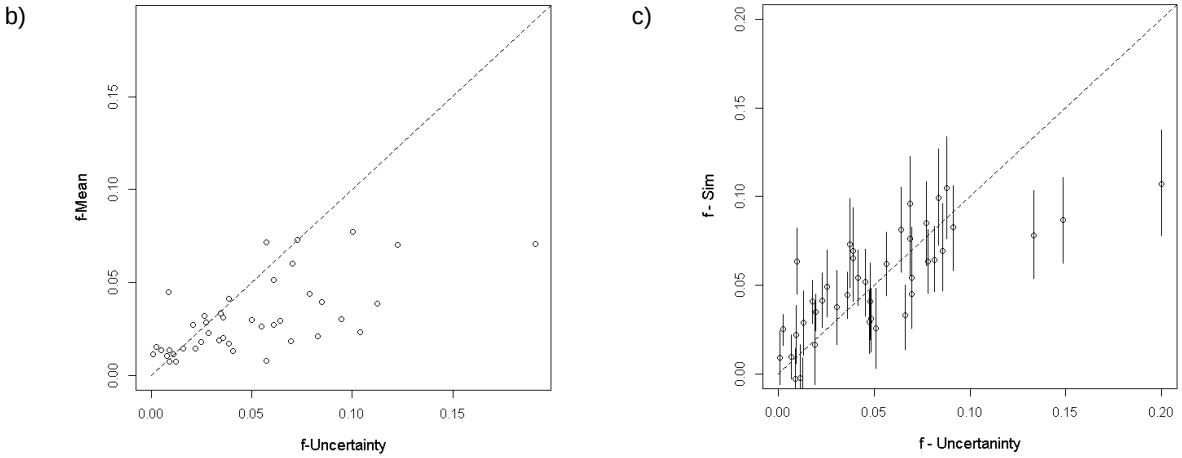

Figure 5. a) Distribution of the predictions of factor f for the 42 tests, using the mean values. Scatter plot of f between b) the estimated to median values with uncertainty and the mean values and c) the prediction of all models and the median of observed with uncertainty.

Figure 5b represents the adjustment of the predictions of all models with the set of mean values and the set of median values with uncertainty. The prediction of the factor, f, performed with the average values is overestimated, given that the equation was calibrated considering the variability of the properties of water and vegetation. Figure 5c represents the adjustment of the predictions of all models with the set of median values obtained from the analysis of propagation of uncertainty. It is noticed that before a set of parameters it is possible to generate the entire distribution of the possible values of the reduction factor of the shear stress on the bed, f, with a confidence interval of 95%. This was achieved after carrying out the analysis of propagation of uncertainty, with which all the sufficient solutions were obtained to represent the distribution of the shear stresses in vegetated flows.

4 CONCLUSIONS

The purpose of this work was to characterize the relative shear stress distribution in vegetated flows based on experimental uncertainty approach. The paper presents the results of a series of experiments with rigid vegetation analyzed with the propagation of uncertainty that allows estimate the distribution of shear stresses with a confidence interval (mean error of 16.07%) in vegetated flows for emergent and submerged hydraulic conditions.

It is found that the contribution of the bed shear stress in the studied vegetated flows not only depends on the vegetation configuration but also on the hydraulic regime. This aspect emphasizes the relevance of the propose the equation, which considers first for the time the interaction between these factors.

In this research the experimental uncertainty approach was applied, which allowed to establish that using the methods without uncertainties can generate errors between 0.1% and 245% and an average error of 62%, compared with the results obtained by considering the propagation of uncertainties. This offers the possibility of developing models that capture the essence of the process and predict more reliable results with an interval of confidence, which reduces the error of the estimates of conventional models that perform a single estimate without a confidence interval. It is important to apply the experimental uncertainty approach in future research since it has established the incidence that it has in the results obtained when compared with the methods with mean values. This approach acquires more importance in fluvial hydraulics given the uncertainty of the measurements and the hydrological variability present in natural channels.

From our experiments, it was possible to develop an equation to estimate the distribution of shear forces determined from an uncertainty propagation analysis and PLS. Thanks to the uncertainty approach used, the model predicts enough values to represent the process with an error in the estimate of 16%. The parameters used within the equation are independent of the flow and represent the characteristics of the vegetation and the channel, which avoids the use of resistance predictors of the bed material in terms of roughness coefficient and speed predictors in the vegetation zone, reducing the error presented by single value estimates. The model used (PLS) is the one that best predicts the distribution of the shear stresses as a function of the independent parameters of the flow, the vegetation properties, the channel slope and the submergence ratio with higher statistical significance: this presented a better performance than the optimization of linear and non-linear equations, support vector machines, among others. It is advisable to carry out further research in which efforts can be measured and directly determine their distribution, to validate the results obtained in this research, because in this study they were determined indirectly from the velocity profiles.

Our experiments emphasize two different patterns in the uncertainty brand of the shear stresses distribution as a function of the submerged ratio. First, the uncertainty increases as the slope grows and second, the uncertainty is greater when the vegetation is emergent and increases when the submergence ratio decreases. Since the uncertainty in previous investigations has not been considered, the results of this investigation allow identifying the conditions in which those models might have a greater error in their prediction. It's important to carry out investigations with experimental setups different from those used in this study, to determine how the distribution of shear forces changes in other configurations not considered in this work.

ACKNOWLEDGMENTS

We thank the Pontificia Universidad Javeriana for supporting research within the framework of proposal #8309 - Estimación de la distribución relativa de esfuerzos de corte en canales con vegetación.

REFERENCES

Aberle, J., Järvelä, J., 2013. Flow resistance of emergent rigid and flexible floodplain vegetation. Journal of Hydraulic Research. 51, 33–45.

Albayrak, I., Nikora, V., Miler, O., O'Hare, M.T., 2014. Flow–plant interactions at leaf, stem and shoot scales: drag, turbulence, and biomechanics. Aquatic Sciences. 76, 269–294.

Baptist, M.J., 2005. Modelling floodplain biogeomorphology. PhD thesis, Delft University of Technology, Civil Engineering and Geosciences Faculty, Delft, The Netherlands.

Chen, Y.-C., Kao, S.-P., 2011. Velocity distribution in open channels with submerged aquatic plant. *Hydrological processes*. 25, 2009–2017.

Cheng, N.-S., 2013. Calculation of drag coefficient for arrays of emergent circular cylinders with pseudofluid model. Journal of Hydraulic Engineering. 139, 602–611.

de Langre, E., Gutierrez, A., Cossé, J., 2012. On the scaling of drag reduction by reconfiguration in plants. Comptes Rendus Mécanique, Biomimetic flow control 340, 35–40.

Dittrich, A., Aberle, J., Schoneboom, T., 2012. Environmental Fluid Mechanics: Memorial colloquium on environmental fluid mechanics in honour of Prof. Gerhard H. Jirka, chapter Drag forces and flow resistabce of flexible riparian vegetation, pages 195-215. IAHR Monographs. CRC Press.

Engineering ToolBox, 2009. Density of Liquids versus change in Pressure and Temperature. Density Specif. Vol. Liq. Change Press. Temp. URL https://www.engineeringtoolbox.com/fluid-density-temperature-pressure-d_309.html (accessed 3.15.19).

Finn, R.K., 1953. Determination of the Drag on a Cylinder at Low Reynolds Numbers. Journal if Applied Physics, 24(6), 771–773.

Freeman, G.E., Rahmeyer, W.H., Copeland, R.R., 2000. Determination of resistance due to shrubs and woody vegetation. Technical report, ERDC/CHL TR-00-25, U.S. Army Engineer Research and Development Center, Vicksburg, MS.

Ghisalberti, M., Nepf, H., 2004. The limited growth of vegetated shear layers. Water Resources Research, 40(7): W0752, doi:10.1029/2003WR002776.

Gosselin, F., Langre, E. de, Machado-Almeida, B.A., 2010. Drag reduction of flexible plates by reconfiguration. Journal of Fluid Mechanics, 650, 319–341.

Guo, J., Zhang, J., 2016. Velocity distributions in laminar and turbulent vegetated flows. *Journal of Hydraulic Research*, *54*, 117-130.

Gurnell, A., 2014. Plants as river system engineers. Earth Surface Processes and Land-forms 39, 4–25.

Hickin, E.J., 1984. Vegetation and river channel dynamics. Canadian Geographer / Le Géographe Canadien, 28(2), 111–126.

Ikeda, S., Kanazawa, M., 1996. Three-dimensional organized vortices above flexible water plants. Journal of Hydraulic Engineering, 122, 634–640.

Järvelä, J., 2004. Determination of flow resistance caused by non-submerged woody vegetation. International Journal of River Basin Management. 2, 61–70.

Kleinhans, M.G., 2010. Sorting out river channel patterns. Progress in Physical Geography. 34, 287–326.

Li, R., Shen, H.W., 1973. Effect of tall vegetations on flow and sediment. Journal of the Hydraulics Division ASCE. 99.

National Oceanic and Atmospheric Administration, 1976. US Standard Atmosphere. Natl. Aeronaut. Space Adm. U. S. Air Force Wash. DC.

Nepf, H.M., 2012. Flow and transport in regions with aquatic vegetation. Annual Review of Fluid Mechanics. 44, 123–142.

Petryk, S., Bosmajian III, G., 1975. Analysis of flow through vegetation. Journal of the Hydraulics Division ASCE. 101.

Serway, R.A., Jewett, J.W., 2018. Physics for scientists and engineers with modern physics. Cengage learning.

Siniscalchi, F., Nikora, V., 2013. Dynamic reconfiguration of aquatic plants and its interrelations with upstream turbulence and drag forces. Jornal of Hydraulic Research. 51, 46–55.

Statzner, B., Lamouroux, N., Nikora, V., Sagnes, P., 2006. The debate about drag and reconfiguration of freshwater macrophytes: comparing results obtained by three recently discussed approaches. Freshwater Biology. 51, 2173–2183.

Tang, H., Tian, Z., Yan, J., Yuan, S., 2014. Determining drag coefficients and their application in modelling of turbulent flow with submerged vegetation. Advances in Water Resources. 69, 134–145.

Thompson, A.M., Wilson, B.N., Hansen, B.J., 2004. Shear stress partitioning for idealized vegetated surfaces. *Transactions of the ASAE*. 47, 701–709.

Tollner, E., Barfield, B., Vachirakornwatana, C., Haan, C., 1977. Sediment deposition patterns in simulated grass filters. Transactions of the ASAE. 20, 940–0944.

Torres, A., Bertrand-Krajewski, J.-L., 2008. Partial least squares local calibration of a UV–visible spectrometer used for in situ measurements of COD and TSS concentrations in urban drainage systems. Water Science and Technology. 57, 581–588.

Torres, A., Lepot, M., Bertrand-Krajewski, J., 2013. Local calibration for a UV/Vis spectrometer: PLS vs. SVM. A case study in a WWTP, in: 7th International Conference on Sewer Processes & Networks. pp. 1–8.

Tritton, D.J., 1959. Experiments on the flow past a circular cylinder at low Reynolds numbers. Journal of Fluid Mechanics. 6, 547–567.

Tsujimoto, T., 1999. Fluvial processes in streams with vegetation. Journal of Hydraulic Research. 37, 789–803.

Vargas-Luna, 2016. A. Role of vegetation on river bank accretion. PhD thesis, Delft University of Technology, Civil Engineering and Geosciences Faculty, Delft, The Netherlands.

Vargas-Luna, A., Crosato, A., Calvani, G., Uijttewaal, W.S.J., 2016. Representing plants as rigid cylinders in experiments and models. Advances in Water Resourses, 93, 205–222.

Vargas-Luna, A., Crosato, A., Uijttewaal, W.S., 2015a. Effects of vegetation on flow and sediment transport: comparative analyses and validation of predicting models. Earth Surface Process and Landforms. 40, 157–176.

Vargas-Luna, A., Crosato, A., Collot, L., Uijttewaal, W., 2015b. Laboratory investigation on the hydrodynamic characterization of artificial grass. In E-proceedings of the 36th IAHR World Congress 28 June-3 July, 2015. The Hague, The Netherlands. ISBN:978-90-824846-0-1., pages 728-734.

Västilä, K., Järvelä, J., Aberle, J., 2013. Characteristic reference areas for estimating flow resistance of natural foliated vegetation. Journal of Hydrology. 492, 49–60.

Velasco, D., Bateman, A., Medina, V., 2008. A new integrated, hydro-mechanical model applied to flexible vegetation in riverbeds. Journal of Hydraulic Research. 46, 579–597.

Wu, W., He, Z., 2009. Effects of vegetation on flow conveyance and sediment transport capacity. International Journal of Sediment Research. 24, 247–259.